Cross-Entropy-based Stationary Proposal Importance Sampling for life-cycle structural reliability and seismic risk assessment

Luca Capacci
Assistant Professor, Dept. of Civil and Environmental Engineering, Politecnico di Milano, Milan, Italy

Fabio Biondini
Professor, Dept. of Civil and Environmental Engineering, Politecnico di Milano, Milan, Italy

ABSTRACT: Life-cycle reliability assessment of deteriorating systems may involve the modeling of complex stochastic processes, further propagating uncertainties and exacerbating computational efforts. This paper discusses a novel simulation-based framework to estimate the time-variant failure probabilities based on Importance Sampling (IS) with Stationary Proposal (SP) distribution. IS methodologies allow to improve computational efficiency and estimate accuracy of simulation-based failure probabilities. The proposed methodology extends adaptive numerical approaches traditionally developed for time-invariant problems, in which the Kullback–Leibler Cross-Entropy is minimized to find a near-optimal simulation density from a chosen family of parametric distributions. The proposed framework is applied to typical reliability problems extended to account for a life-cycle perspective and time-variant seismic risk of deteriorating bridge networks.

1. INTRODUCTION

Monte Carlo simulation (MCS) is a viable tool to solve large-scale reliability and risk analysis problems. Its feasibility can be limited in practice when intensive numerical analyses are required to estimate small probabilities over complex failure domains, such as seismic risk analysis of infrastructure networks (Messore et al. 2021). Life-cycle assessment of deteriorating systems may also involve the modeling of complex stochastic processes, further exacerbating the computational effort (Yang et al. 2017). Incorporating aging effects and cumulative damage into standard computational procedures is an open issue in reliability assessment of stand-alone structures and seismic vulnerability of large-scale systems (Silva et al. 2019, Capacci and Biondini 2022a).

In this paper, a novel simulation-based framework for life-cycle structural reliability and risk assessment is proposed based on Importance Sampling with Stationary Proposal distribution (SP-IS). This is a variance reduction technique formulated to improve the trade-off between computational efficiency and estimate accuracy. Random variables and stochastic processes are efficiently sampled from a time-invariant distribution, whilst the reliability estimates are defined by weighting each failed sample based on its evolving likelihood of occurrence over the target lifetime. The proposed numerical approach relies on the selection of a near-optimal simulation density adaptively identified by minimizing the Kullback–Leibler (KL) Cross-Entropy (CE), which is a measure of the discrepancy between a target sampling function and a parametric density distribution of a preselected family (Rubinstein 1981). The proposed CE-based framework is numerically investigated for typical structural reliability problems extended to a life-cycle perspective. The methodology is then applied to estimate time-variant risk metrics, such as the mean annual rate of target resilience exceedance, for a small-scale deteriorating bridge network. Estimate accuracy and computational effort are investigated in comparison with traditional simulation approaches.

2. STATIONARY PROPOSAL IMPORTANCE SAMPLING (SP-IS)

2.1. Time-variant failure probability

In life-cycle structural reliability and risk assessment, the effects of uncertainties are time-variant due to mechanical and deterioration processes. The evolution in time of structural capacity and demand are related to stochastic processes $\mathbf{X}(t)$ generated based on the structural model (e.g., material properties, geometry, loadings, among others), as well as on deterioration indices describing the degradation in time of the structure.

Simulation methods are intended to numerically estimate the probability of event occurrence based on the formulation of a multidimensional integral, such as the mathematical expectation of the failure indicator function I in terms of a set of Random Variables (RVs) $\mathbf{X}$ characterized by the time-variant joint Probability Density Function (PDF) $f_{\mathbf{X}}(\mathbf{x})$:

$$P_f(t) = E_{f_{\mathbf{X}(t)}}[I(\mathbf{x})] = \int_{\mathbf{x}} I(\mathbf{x}) \cdot f_{\mathbf{X}(t)}(\mathbf{x}) d\mathbf{x} \quad (1)$$

The indicator I is a Heaviside step function equal to 1 in the failure domain described by $\{g(\mathbf{x}) \leq 0\}$, where $g(\mathbf{x})$ is the limit state function, and equal to 0 in the safe domain.

2.2. Importance sampling estimate

The aim of Importance Sampling (IS) is to improve the accuracy of reliability estimates by reformulating the failure probability in terms of an alternative sampling distribution $\psi(\mathbf{x})$, also referred to as proposal or sampling distribution:

$$P_f(t) = \int_{\mathbf{x}} I(\mathbf{x}) \cdot f_{\mathbf{X}(t)}(\mathbf{x}|t) \cdot \frac{\psi(\mathbf{x})}{\psi(\mathbf{x})} d\mathbf{x} \quad (2)$$

The IS reformulation of the failure probability relies on the IS weighting coefficient W defined as the ratio between the actual *time-variant* PDF $f_{\mathbf{X}(t)}$ and the sampling *time-invariant* PDF ψ:

$$W(\mathbf{x}|t) = \frac{f_{\mathbf{X}(t)}(\mathbf{x})}{\psi(\mathbf{x})} \quad (3)$$

The time-variant IS failure probability corresponds to the mathematical expectation in terms of the sampling PDF of the product between indicator function I and coefficients W:

$$P_f(t) = E_{\psi}[I(\mathbf{x}) \cdot W(\mathbf{x}|t)] \quad (4)$$

The failure probability can also be formulated based on the multidimensional integral as follows:

$$P_f(t) = \int_{\mathbf{x}} I(\mathbf{x}) \cdot W(\mathbf{x}|t) \cdot \psi(\mathbf{x}) d\mathbf{x} \quad (5)$$

The IS failure probability estimator is the weighted sample mean of the indicator function with sample size N:

$$p_{IS}(t) = \frac{1}{N} \sum_{i=1}^{N} I_i \cdot w_i(t) \quad (6)$$

The weighting coefficient is the sample time-variant coefficient $w_i(t)=W(\mathbf{x}_i|t)$ evaluated for the i-th simulated set of basic RVs $\mathbf{x}_i$ at time t. The variance of the IS estimator is evaluated as follows (Capacci and Biondini 2021):

$$\sigma_{IS}^2(t) \approx \frac{1}{N-1} \left\{ \frac{1}{N} \sum_{i=1}^{N} [I_i \cdot w_i^2(t)] - p_{IS}^2(t) \right\} \quad (7)$$

In traditional MCS, samples generation is based on a distribution progressively evolving within the sample space over the system lifetime, requiring one simulation per observation time t. On the other hand, SP-IS involves a single simulation to estimate probabilities at different times t by suitably weighting each failed sample. The choice of the sampling density ψ is a key issue in the SP-IS framework to effectively improve the trade-off between accuracy and sample size.

3. CROSS-ENTROPY-BASED OPTIMAL DISTRIBUTION (CE-SP-IS)

3.1. Kullback-Leibler (KL) cross-entropy (CE) minimization

Minimizing the IS estimate variance effectively improves the simulation performance. The aim of methodologies based on Cross-Entropy (CE) is to formulate a near-optimal simulation density from a chosen family of parametric distributions. The Kullback-Leibler Cross-Entropy (KL-CE) measures the discrepancy between a prescribed distribution and the absolute best sampling density (Rubinstein 1981). The KL-CE between the best possible density p^* and a prescribed proposal PDF ψ with parameters **v** is expressed as:

$$D_{KL} = \int_{\mathbf{x}} p^*(\mathbf{x}) \cdot \ln p^*(\mathbf{x})\, d\mathbf{x} - \\ - \int_{\mathbf{x}} p^*(\mathbf{x}) \cdot \ln \psi(\mathbf{x}, \mathbf{v})\, d\mathbf{x} \tag{8}$$

The proposal parameters **v** minimizing the cross-entropy are obtained by formulating an optimization problem that maximizes the second term in D_{KL} (i.e., the only term where **v** appears):

$$\text{argmin}_{\mathbf{v}} D_{KL} = \\ = \text{argmax}_{\mathbf{v}} \int_{\mathbf{x}} \frac{I(\mathbf{x}) \cdot f_{\mathbf{X}}(\mathbf{x})}{P_f} \cdot \ln \psi(\mathbf{x}, \mathbf{v})\, d\mathbf{x} \tag{9}$$

where p^* corresponds to the density of the random RVs censored based on the indicator function $I(\mathbf{x})$ and normalized by the target failure probability P_f.

The optimization problem is solved by decoupling the target parameters **v** of the near-optimal distribution from the iteratively updated parameters **w** of the sampling density. The basic RVs distribution $f_{\mathbf{X}}(\mathbf{x})$ in the integrand function of Equation (9) is accommodated by exploiting the definition of IS analytically defined as $W(\mathbf{x},\mathbf{w})=f_{\mathbf{X}}(\mathbf{x})/\psi(\mathbf{x},\mathbf{w})$ in order to introduce an alternative distribution $\psi(\mathbf{x},\mathbf{w})$ of the same family of $\psi(\mathbf{x},\mathbf{v})$:

$$\text{argmin}_{\mathbf{v}} D_{KL} = \\ = \text{argmax}_{\mathbf{v}} \int_{\mathbf{x}} \frac{I(\mathbf{x}) \cdot W(\mathbf{x},\mathbf{w}) \cdot \psi(\mathbf{x},\mathbf{w})}{P_f} \ln \psi(\mathbf{x}, \mathbf{v})\, d\mathbf{x} = \\ = \text{argmax}_{\mathbf{v}} E_{\psi(\mathbf{x},\mathbf{w})}\left[\frac{I(\mathbf{x}) \cdot w(\mathbf{x},\mathbf{w})}{P_f} \ln \psi(\mathbf{x}, \mathbf{v})\right] \tag{10}$$

The statistical parameters in **w** are iteratively updated by estimating the expectation based on the generation of N samples of the basic RVs $\mathbf{x}_i$ from the sampling distribution $\psi(\mathbf{x},\mathbf{w})$. Assuming $P_f \approx p_{IS}$, the optimization problem can be formulated as:

$$\text{argmin}_{\mathbf{v}} D_{KL} \approx \\ \approx \text{argmax}_{\mathbf{v}} \frac{1}{N} \sum_{i=1}^{N} \left[\frac{I_i \cdot w_i(\mathbf{w})}{p_{IS}} \ln \psi_i(\mathbf{v})\right] \tag{11}$$

where $w_i(\mathbf{w})=w(\mathbf{x}_i,\mathbf{w})$ and $\ln\psi_i(\mathbf{v})=\ln\psi(\mathbf{x}_i,\mathbf{v})$. When the function is concave and differentiable with respect to **v**, the near-optimal density can be obtained by setting the gradient to zero:

$$\frac{1}{N} \sum_{i=1}^{N} \widetilde{w}_i(\mathbf{w}) \cdot [\nabla_{\mathbf{v}} \ln \psi_i(\mathbf{v})] = 0 \tag{12}$$

with the i-th weight $\widetilde{w}_i$ defined as follows:

$$\widetilde{w}_i(\mathbf{w}) = \frac{I_i \cdot w_i(\mathbf{w})}{p_{IS}} \tag{13}$$

3.2. CE-SP-IS optimal densities

In the SP-IS approach, the best possible density $p^*(\mathbf{x})$ can be defined over the time horizon of the life-cycle reliability analysis at n_t discrete times t:

$$p^*(\mathbf{x}) = \frac{1}{n_t}\left[\sum_{z=1}^{n_t} \frac{I(\mathbf{x}) \cdot f_{\mathbf{X}(t_z)}(\mathbf{x}|t_z)}{P_f(t_z)}\right] \tag{14}$$

The same rationale can be applied to define the optimal densities considering n_s limit state functions and n_p parametric hazard scenarios:

$$p^*(\mathbf{x}) = \frac{1}{n_s}\left[\sum_{s=1}^{n_s} \frac{I(\mathbf{x}|s) \cdot f_{\mathbf{X}}(\mathbf{x})}{P_f(s)}\right] \tag{15}$$

$$p^*(\mathbf{x}) = \frac{1}{n_p}\left[\sum_{p=1}^{n_p} \frac{I(\mathbf{x}) \cdot f_{\mathbf{X}(p)}(\mathbf{x}|p)}{P_f(h)}\right] \tag{16}$$

The formulation of the best density can account for n_c combinations of the n_t time instants for n_s limit states and n_p hazard scenarios:

$$p^*(\mathbf{x}) = \frac{1}{n_c}\left[\sum_{c=1}^{n_c} \frac{I(\mathbf{x}|c) \cdot f_{\mathbf{X}(c)}(\mathbf{x}|c)}{P_f(c)}\right] \tag{17}$$

Substituting this density into Equation (8) leads to the same solving system in Equation (12) and the updating coefficients $\widetilde{w}_i$ are arranged as follows:

$$\widetilde{w}_i(\mathbf{w}) = \frac{1}{n_c} \sum_{c=1}^{n_c} \frac{I_i(s) \cdot w_i(\mathbf{w}|t_z,p)}{p_{IS}(c)} \tag{18}$$

where $p_{IS}(c)$ is the failure probability estimate for the c-th combination of time t_z, scenario h and limit state s. Indicator functions I_i are independent from time and hazard scenario, whilst weighting coefficients w_i do not depend on the limit state.

3.3. Updating rules for Gaussian Mixture (GM)

Among all families of parametric distributions, Gaussian Mixtures (GMs) can efficiently map the most significant regions in the failure domain. The proposal distribution $\psi(\mathbf{x},\mathbf{v})$ is composed by K Gaussian variates:

$$\psi(\mathbf{x},\mathbf{v}) = \sum_{k=1}^{K} \pi_k \cdot N(\mathbf{x}|\boldsymbol{\mu}_k,\boldsymbol{\Sigma}_k) \tag{19}$$

where $N(\mathbf{x}|\boldsymbol{\mu}_k,\boldsymbol{\Sigma}_k)$ is the k-th joint normal PDF with weighting probability π_k, mean vector $\boldsymbol{\mu}_k$, covariance matrix $\boldsymbol{\Sigma}_k$,.

Substituting the IS density in Equation 12, the CE minimization problem is reformulated with exponential densities and explicit updating rules for **w** can be adopted to iteratively solve it (Rubinstein and Kroese 2004). At the (m+1)-th iteration and for the k-th Gaussian density in the mixture model, the updating rules are:

$$\pi_k^{(m+1)} = \frac{\sum_{i=1}^{N} \tilde{w}_i \cdot \gamma_{ik}^{(m)}}{\sum_{i=1}^{N} \tilde{w}_i} \tag{20}$$

$$\boldsymbol{\mu}_k^{(m+1)} = \frac{\sum_{j=1}^{N} \tilde{w}_i \cdot \gamma_{ik}^{(m)} \cdot \mathbf{x}_i}{\sum_{j=1}^{N} \tilde{w}_j \cdot \gamma_{ik}^{(m)}} \tag{21}$$

$$\boldsymbol{\Sigma}_k^{(m+1)} = \frac{\sum_{i=1}^{N} \tilde{w}_i \cdot \gamma_{ik}^{(m)} \cdot \left(\mathbf{x}_i - \boldsymbol{\mu}_k^{(m)}\right) \cdot \left(\mathbf{x}_j - \boldsymbol{\mu}_k^{(m)}\right)^{\mathrm{T}}}{\sum_{i=1}^{N} \tilde{w}_i \cdot \gamma_{ik}^{(m)}} \tag{22}$$

where the parameter γ_{ik} is the i-th sample responsibility of the k-th marginal Gaussian, representing the assignment of each sample to the k-th density (Kurtz and Song 2013):

$$\gamma_{ik}^{(m)} = \frac{\psi_k(\mathbf{x}_i)}{\psi(\mathbf{x}_i)} = \frac{\pi_k^{(m)} \cdot N\left(\mathbf{x}_i|\boldsymbol{\mu}_k^{(m)},\boldsymbol{\Sigma}_k^{(m)}\right)}{\sum_{k=1}^{K} \pi_k^{(m)} \cdot N\left(\mathbf{x}_i|\boldsymbol{\mu}_k^{(m)},\boldsymbol{\Sigma}_k^{(m)}\right)} \tag{23}$$

The CE optimization problem is also equivalent to the Maximum Likelihood Estimate of the mixture parameters and the GM parameters update can be further refined via expectation-maximization algorithms (Geyer et al. 2019).

4. BASIC NUMERICAL APPLICATION

The presented approach is firstly applied to a basic example of time-variant reliability analysis inspired by a traditional reliability problem with multiple design points associated with a parabolic limit state function (Der Kiureghian and Dakessian 1998):

$$g(\mathbf{X}) = b - X_2 - \kappa(X_1 - e)^2 \tag{24}$$

The statistical parameters of **X** are assumed to vary over the normalized time τ. In pristine conditions (i.e., τ=0), the basic RVs **X** are standard normal and statistically independent. The deterioration process is described by n_p=3 combinations of quadratic variation of the mean value of X_1 and a linear increase of the standard deviation of X_2:

$$\mu_1(t) = \chi_1 \cdot \tau^2 \tag{25}$$

$$\sigma_2(t) = 1 + \chi_2 \cdot \tau \tag{26}$$

The damage scenarios are characterized by the evolution of (1) only μ_1 with χ_1=3, (2) only σ_2 with χ_2=1, and (3) both μ_1 and σ_2 with χ_1=3 and χ_2=1.

The optimal proposal density is identified considering multiple time instants n_t, limit states n_s and parametric hazard scenarios n_p. Reliability is assessed for n_t=21 normalized time instants (i.e., from 0.00 to 1.00 every 0.05). The n_s=6 parabolic limit state functions shown in Figure 1 are characterized by null eccentricity (e=0) and vertices b=8.0 (thick lines) and b=5.0 (thin lines). Dotted, dashed, and continuous lines refer to curvatures κ=0.00, 0.05, and 0.10, respectively. The number of reliability problems to be solved is $\underline{n_c}=\underline{n_t}\cdot\underline{n_s}\cdot\underline{n_p}$=378.

Figure 1 also shows the contour plots of the initial GM model constituted by n_k=10 binormal densities each with probability π_k=1/n_k. To efficiently map the sample space, the mean vectors $\boldsymbol{\mu}_k$ (square markers) are randomly simulated from a normal uncorrelated bivariate distribution centered at the space origin and with standard deviation σ=3. Also, the covariance matrices $\boldsymbol{\Sigma}_k$ are initialized with null correlation and standard deviations σ_k=3. The initial phase of the near-optimal GM density comprises of four rounds n_{iter}=4 of pre-sampling with N_{pre}=5000 samples. Given the descriptors collected in Table 1, the final simulation is carried out on N_{final}=80000 samples, for a total number of $n_{iter}\cdot N_{pre}+N_{final}=10^5$ samples. Figure 2 shows the limit state functions (black opaque lines) and the samples (grayscale dots) generated by the final GM proposal density (white contour plot).

Figure 3 presents the estimated time-variant reliability indices β ranging from 1.4 to 8.0. The estimates CoV in Figure 4 show accurate results for all reliability problems, with average and maximum values respectively 2.1% and 4.7%.

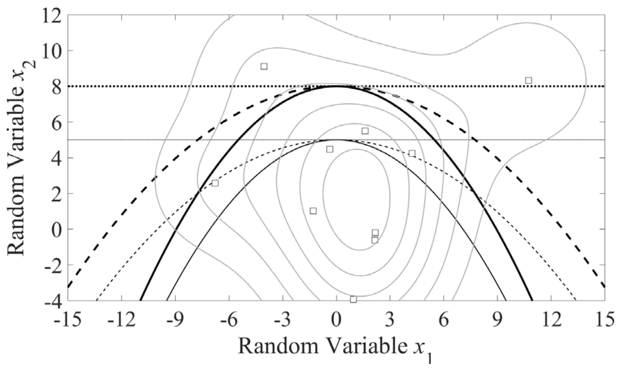

Figure 1: Limit states and initial GM densities.

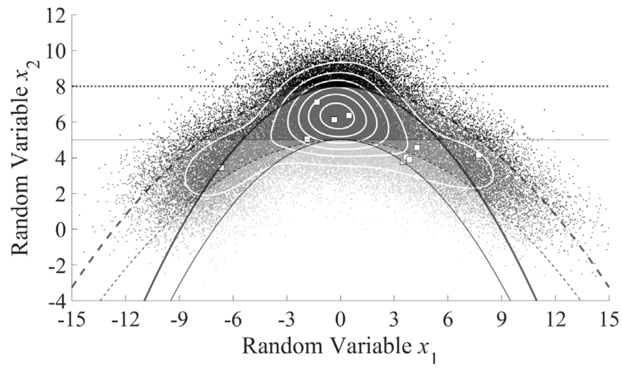

Figure 2: CE-SP-IS density and simulated samples.

Table 1: Statistical parameters calibrated by CE-SP-IS for each bivariate density in the GM.

$\mathbf{v}_k$	k=1	k=2	k=3	k=4	k=5	k=6	k=7	k=8	k=9	k=10
μ_1	+0.478	–6.672	+3.502	–1.857	+7.706	–1.306	+3.674	+3.859	–0.355	+4.270
μ_2	+6.352	+3.448	+3.790	+5.048	+4.127	+7.122	+4.033	+3.902	+6.140	+4.580
σ_1	1.400	1.429	2.165	1.720	1.269	1.459	1.900	1.902	1.321	1.833
σ_2	1.229	1.274	1.334	1.066	1.174	1.193	1.287	1.300	1.192	1.433
ρ_{12}	–0.255	+0.425	–0.710	+0.542	–0.537	+0.543	–0.788	–0.798	+0.154	–0.710
π	0.200	0.147	0.003	0.070	0.031	0.120	0.041	0.033	0.210	0.145

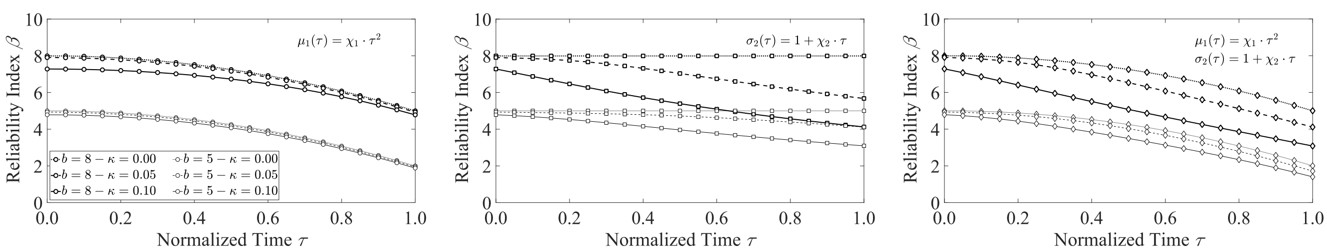

(a) (b) (c)

Figure 3: Reliability indices for all limit states with time-variant (a) μ_1, (b) σ_2, (c) both μ_1 and σ_2.

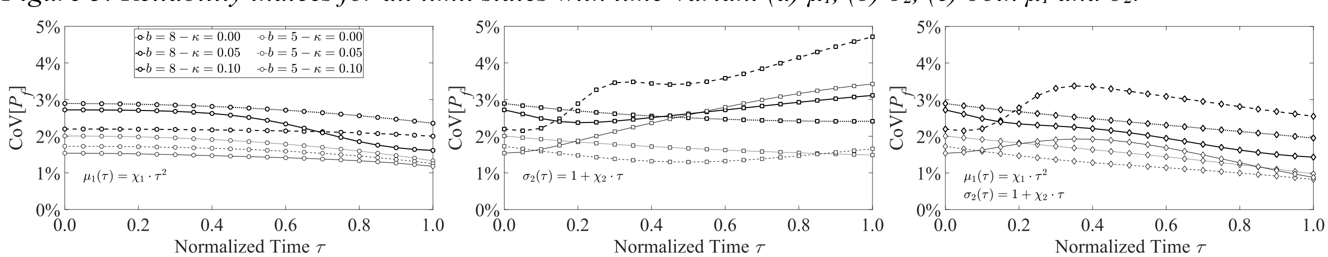

(a) (b) (c)

Figure 4: Failure probability CoV for all limit states with time-variant (a) μ_1, (b) σ_2, (c) both μ_1 and σ_2.

5. LIFE-CYCLE SEISMIC RISK OF AN AGING BRIDGE NETWORK

5.1. Case study

The road infrastructure network with n_b=3 aging bridges shown in Figure 5 is considered (Capacci and Biondini 2022b). The network is composed by three nodes originating and attracting daily road users' trips connected by main highways, each one with an aging vulnerable bridge, as well as secondary detour roads. Life-cycle seismic risk analysis is carried out based on probabilistic seismic hazard assessment, time-variant bridge fragility curves, and network performance metrics based on the concept of infrastructure resilience (Capacci et al. 2022).

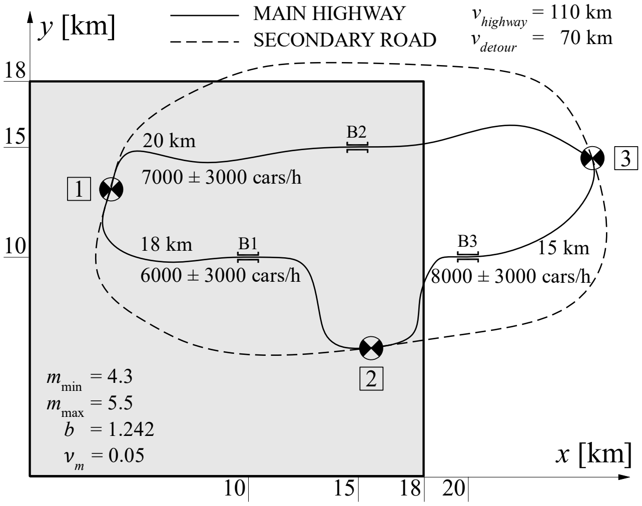

Figure 5: Investigated bridge network.

5.2. Probabilistic seismic hazard

Major seismic events are equally likely to occur throughout the area source represented in Figure 5. The epicenter location $\mathbf{X}_e=\{X,Y\}_e$ is described by a bivariate uncorrelated uniform distribution. The recurrence of earthquakes with severe macroseismic intensity is expressed based on the Gutenberg-Richter distribution in terms of moment magnitude M_w:

$$F_{M_w}(m) = \frac{1-10^{-b(m-m_{\min})}}{1-10^{-b(m_{\max}-m_{\min})}} \qquad (27)$$

with parameters collected in Figure 5.

The Peak Ground Acceleration (PGA) is herein selected as seismic intensity measure at the b-th bridge site I_b [g] and it is defined based on a joint lognormal model. The median seismic intensity $I_{b,m}$ is generally defined conditional to source-to-site distance $R_{eb}=\|\mathbf{X}_e-\mathbf{X}_b\|$ and moment magnitude M_w. Uncertainties in ground motion intensities are accounted by the within-event joint standard normal correlated variate ε_{W_b} and the between-event single standard normal variate ε_B:

$$\ln I_b = \ln I_{b,m} + \sigma_W \varepsilon_{W_b} + \sigma_B \varepsilon_B \qquad (28)$$

where σ_W and σ_B are the within- and between-event standard deviations, respectively. Median intensity and statistical parameters of the attenuation law are selected from the prediction model proposed in Bindi et al. (2011) with soil of type C based on Eurocode 8 classification and normal faulting. Finally, the within-event correlation is assumed to depend on the relative distance $r_{b_h b_k}$ between h-th and k-th bridges:

$$\rho_{b_h b_k} = \exp\left(-\frac{r_{b_h b_k}}{10}\right) \qquad (29)$$

5.3. Time-variant bridge fragility

The definition of bridge seismic capacities $\bar{I}_b$ relies on the concept of fragility curves, which represent the failure probability conditional to the seismic intensity at the bridge site. The life-cycle seismic fragility of the three spatially-distributed vulnerable aging bridges in the network is described by statistically independent time-variant lognormal models. In the investigated case study, it is assumed that the median seismic capacity $\bar{\iota}_{b,m}$ deteriorates in time due to environmental aging. The degradation law is:

$$\bar{\iota}_{b,m}(t) = \bar{\iota}_{b,m0} - k_b \cdot t^2 \qquad (30)$$

Respectively for bridges B1–B2–B3, the pristine median capacities $\bar{\iota}_{b,m0}$ are 0.7–0.8–0.9g and decay rate parameters k_b are 15–18–25×10^{-5} g/years^2. The standard deviation of the logarithm of the seismic capacity is ζ=0.60 for all bridges.

5.4. Network resilience

Traffic flows f_{OD} in the network are generated by daily trips of road users from Origin nodes O to Destination nodes D. Travel times t_{OD} are assigned by shortest path analysis based on the network topology. Seismic events may lead to bridge closure due to structural collapse, affecting the network performance and increasing the road users' Total Travel Time TTT:

$$TTT = \textstyle\sum_O \sum_D f_{OD} \cdot t_{OD}\,(\mathbf{S}) \qquad (31)$$

where the Boolean random vector $\mathbf{S}$ represents the undamaged and fully operational bridge state S_b=0 and the collapsed and fully closed condition S_b=1. Daily traffic demands f_{OD} are modeled as statistically independent symmetric triangular distributions over the range $f_{OD}^{mode} \pm$ 1500 cars/hour. Traffic demands are perfectly correlated over the same OD pair (e.g., f_{12}=f_{21}). Figure 5 collects all information regarding road lengths, speed limits and traffic flow modes.

Repair activities allow releasing traffic restrictions when the bridge load-bearing capacity is restored. Resilience is expressed as the integral mean of the functionality profile from the time of earthquake occurrence t_0 to a fixed horizon time t_h (Capacci et al. 2020):

$$R = \frac{1}{t_h - t_0} \int_{t_0}^{t_h} Q(t;\mathbf{S})dt \tag{32}$$

where the functionality Q is given by the ratio between the *TTT* in unrestricted conditions (i.e., $\mathbf{S}=\mathbf{0}$) and the *TTT* given the bridge damage combination. Uniform RVs between 230 and 330 are assumed to characterize the probabilistic model for the recovery times $T_{r,b}$ for each bridge. Further insight on the resilience model is reported in Capacci and Biondini (2021, 2022b).

Finally, life-cycle seismic risk is quantified based on the mean annual rate of exceedance of a prescribed resilience target r:

$$\nu_r(r,t) = \nu_m \cdot P[R(t) \leq r] \tag{33}$$

where ν_m is the earthquake occurrence mean annual rate. The numerical estimate of the resilience measure R involves 16 basic RVs: bivariate epicenter location $\mathbf{X}_e$, moment magnitude M_w, within-event variates ε_{W_b}, between-event variate ε_B, seismic capacities $\bar{I}_b$, OD traffic flows f_{OD}, recovery times $T_{r,b}$.

5.5. CE-SP-IS life-cycle seismic risk estimates

The CE-SP-IS method is applied to estimate the resilience CDF at r=60% to 80% every 5% (i.e., n_s=5) from pristine conditions up to 50 years of lifetime every two years (i.e., n_t=26). The total number of combinations is $n_c=n_t \cdot n_s$=130.

The procedure is initialized by selecting a single Gaussian density as sampling distribution with standard parameters (i.e., null mean vector and diagonal unitary covariance matrix). Since most variables are not normally distributed, samples of the basic RVs are simulated in such space $\mathbf{u}_i$ (i.e., simulation space) and then transformed into their actual space $\mathbf{x}_i$ (i.e., analysis space) to compute the indicator functions I_i. Weighting coefficients w_i are computed in the simulation space to retrieve the failure probability estimates p_{IS} and the weights $\tilde{w}_i$ involved in the updating rules.

Figure 6 shows the CE-SP-IS numerical estimates of the mean annual rate of failure to meet the resilience target. Results are obtained with five rounds n_{iter}=5 of pre-sampling with N_{pre}=50000 and final simulation with N_{final}=750000, for a total of 10^6 samples of the basic RVs. The comparison with traditional MCS evaluated every 10 years is carried out with comparable sample sizes. The actual computational cost of MCS should account for the number of observation time instants n_t=6. Thus, the sample size for MCS simulation is set to N=166,667. The MCS estimate for r=60% in pristine conditions (i.e., t_0=0) is not reported since all samples are on the safe domain.

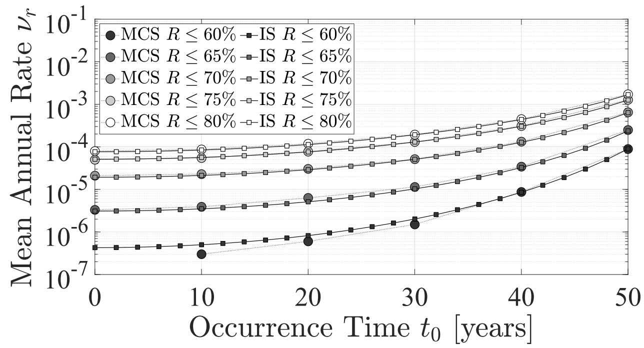

Figure 6: Life-cycle seismic risk estimates.

The estimates CoV in Figure 7 indicate how CE-SP-IS outperforms MCS for almost all investigated combinations of time instant and resilience target. The maximum CoV is 3.4% for r=60% in pristine conditions. All CE-SP-IS estimates have comparable accuracies with average CoV=2.2%.

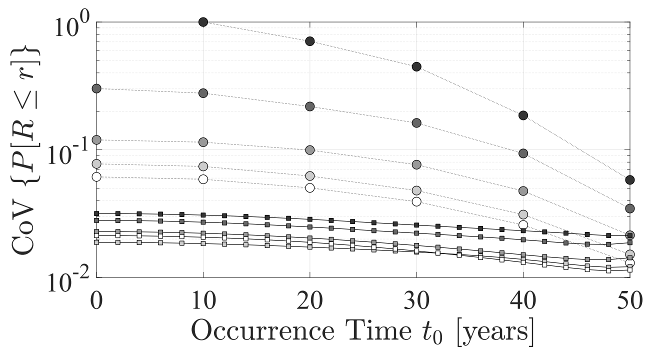

Figure 7: CoV of Life-cycle seismic risk estimates.

6. CONCLUSIONS

The paper presented a novel computational framework to efficiently estimate time-variant structural reliability and life-cycle seismic risk of bridge networks based on Stationary Proposal Importance Sampling (SP-IS). The adaptive technique is used to establish near-optimal sampling Gaussian mixture densities by minimizing the Kullback–Leibler Cross-Entropy (KL-CE) with respect to the best importance sampling density for a combination of reliability problems involving different limit state functions and distributions of basic random variables. The potentialities of the proposed efficient sampling method would emerge when time-consuming analyses are required to assess the limit state functions. Potentially fruitful fields of application regard the development of parametric analyses on the basic random variables such as reliability-based design optimization within a life-cycle framework. A major drawback of the IS methodology is the tendency to produce inefficient probability estimates when large set and wide range of variables are involved in the sampling procedure. Further research should be devoted to address the feasibility limitations of CE-SP-IS approaches in large-scale problems with complex deterioration patterns.

7. REFERENCES

Bindi, D., Pacor, F., Luzi, L., Puglia, R., Massa, M., Ameri, G., & Paolucci, R. (2011). Ground motion prediction equations derived from the Italian strong motion database. *Bulletin of Earthquake Engineering, 9(6)*, 1899–1920.

Capacci, L., Biondini, F., & Titi, A. (2020). Lifetime seismic resilience of aging bridges and road networks. *Structure and Infrastructure Engineering, 16*(2), 266–286.

Capacci, L. & Biondini, F. (2021). Importance sampling in life-cycle seismic fragility and risk assessment of aging bridge networks. *1st Conference of the European Association on Quality Control of Bridges and Structures* (EUROSTRUCT 2021). August 29–September 1, 2021, Padua, Italy.

Capacci, L., & Biondini, F. (2022a). Efficient sampling techniques for simulation-based life-cycle structural reliability and seismic fragility assessment. *13th International Conference on Structural Safety and Reliability* (ICOSSAR 2021), September 13–17, 2022, Shanghai, China.

Capacci, L., Biondini, F. (2022b). Stationary Proposal Importance Sampling (SP-IS) for life-cycle resilience-based seismic risk assessment of deteriorating bridge networks. In: *3rd European Conference on Earthquake Engineering and Seismology* (3ECEES). September 4–9, 2022, Bucharest, Romania.

Capacci, L., Biondini, F., & Frangopol, D. M. (2022). Resilience of aging structures and infrastructure systems with emphasis on seismic resilience of bridges and road networks. *Resilient Cities and Structures*, *1*(2), 23-41.

Der Kiureghian A., & Dakessian T. (1998). Multiple design points in first and second-order reliability. *Structural Safety*, *20*(1):37–49

Geyer, S., Papaioannou, I., & Straub, D. (2019). Cross entropy-based importance sampling using Gaussian densities revisited. *Structural Safety*, *76*, 15-27.

Kurtz, N., & Song, J. (2013). Cross-entropy-based adaptive importance sampling using Gaussian mixture. *Structural Safety, 42*, 35-44.

Messore, M.M., Capacci, L., Biondini, F. (2021). Life-cycle cost-based risk assessment of aging bridge networks. *Structure and Infrastructure Engineering, 17*(4), 515-533.

Rubinstein R. (1981). *Simulation and the Monte Carlo methods.* Hoboken (NJ): John Wiley and Sons, Inc.

Rubinstein R., & Kroese D (2004). *The cross-entropy method: a unified approach to combinatorial optimization, Monte-Carlo Simulation, and machine learning*. New York (NY): Springer, Inc.

Silva, V., Akkar, S., Baker, J. W., Bazzurro, P., Castro, J. M., Crowley, H., Dolsek, M., Galasso, C., Lagomarsino, S., Monteiro, R., Perrone, D., Pitilakis, K., & Vamvatsikos, D. (2019). Current challenges and future trends in analytical fragility and vulnerability modelling. *Earthquake Spectra*, *35*(4), 1927-1952.

Yang, D. Y., Teng, J. G., & Frangopol, D. M. (2017). Cross-entropy-based adaptive importance sampling for time-dependent reliability analysis of deteriorating structures. *Structural Safety*, *66*, 38-50.